Journal of Power Sources 195 (2010) 8044–8051

Contents lists available at ScienceDirect

Journal of Power Sources

journal homepage: www.elsevier.com/locate/jpowsour

Performance enhancement of air-breathing proton exchange membrane fuel cell through utilization of an effective self-humidifying platinum–carbon catalyst

Chee Kok Poh[a,b], Zhiqun Tian[a], Narissara Bussayajarn[c], Zhe Tang[d], Fabing Su[e], San Hua Lim[a], Yuan Ping Feng[b], Daniel Chua[d], Jianyi Lin[a,b,*]

[a] Institute of Chemical Engineering and Sciences, 1 Pesek Road, Jurong Island, Singapore 627833, Singapore
[b] Department of Physics, National University of Singapore, Singapore 117542, Singapore
[c] Singapore Institute of Manufacturing Technology, 71 Nanyang Drive, Singapore 638075, Singapore
[d] Department of Materials Science and Engineering, National University of Singapore, Singapore, Singapore
[e] State Key Laboratory of Multi-phase Complex System, Institute of Process Engineering, Chinese Academy of Sciences, Beijing 100190, China

ARTICLE INFO

Article history:
Received 26 March 2010
Received in revised form 1 June 2010
Accepted 11 June 2010
Available online 8 July 2010

Keywords:
Functionalization
Pt nanoparticles
Self-humidifying
Fuel cells
Citric acid

ABSTRACT

One issue with air-breathing proton exchange membrane fuel cells (AB-PEMFCs) is that the reactants are not externally humidified, and thus the membrane or the catalyst layers might dry out due to electro-osmotic drag, diffusion and evaporation at the opening cathode. This results in a drop in internal ionic conductivity and thus in cell performance. Here, the preparation and characterization of self-humidifying carbon-supported Pt catalyst using citric acid modified carbon black (CA-CB) as the catalyst support are reported. Pt/CA-CB is highly hydrophilic due to the functional groups attached on the carbon support, which endows the ability to retain water in the membrane electrolyte assembly (MEA) and thereby help to improve the performance of AB-PEMFCs. A maximum power density of 204 mW cm^{-2} can be achieved in an air-breathing PEMFC stack using Pt/CA-CB, a thick polymer membrane (NRE212) and a circular opening cathode. A 23.4% enhancement in the output power density is obtained by using Pt/CA-CB in place of a commercial catalyst when oblique slit cathodes are employed. This self-humidifying catalyst is particularly suitable for portable PEMFC applications.

1. Introduction

The advantages of proton exchange membrane fuel cells (PEMFCs), such as low operating temperature, quick start-up and high specific energy make them highly suitable for portable applications. Dyer [1] concluded that the cost tolerance (which is the allowable cost based on the competitive technology to be displaced or complemented) for fuel cells in portable devices is two orders of magnitude greater than that for automotive applications. Thus PEMFCs manufacturing and sales for portable applications have exhibited stronger market growth than their production for other applications in the past few years.

Air-breathing proton exchange membrane fuel cells (AB-PEMFCs) are commonly used for portable applications. One issue with AB-PEMFCs is that the reactants are not externally humidified, and thus the membrane or the catalyst layers are found to dry out due to water electro-osmotic drag, back diffusion or evaporation at the opening cathode [2]. Self-humidifying MEAs are deemed to be the solution to this problem [2–8]. To fabricate self-humidifying MEAs, modifications of the membrane were undertaken by adding hygroscopic materials such as silica and zirconia particles [2], or Pt catalyst materials (for water production) [3–5], or adding both materials [6–8]. The modification of a membrane using a Pt catalyst is costly, and might create electron-conducting paths that increase the possibility of a short-circuit through the membrane. To avoid this, a composite membrane with a sandwich structure was proposed [5], but the fabrication of a sandwich structure with a Pt catalyst is still expensive. Another way to solve the problem was to modify the electrodes where hygroscopic material such as SiO_2 was added to the electrodes instead of modifying the membrane to increase the water content in the MEA and reduce the ionic resistance in the cell [9,10]. Recently Eastcott and Easton [11] produced a ceramic carbon electrode where SiO_2 was homogeneously distributed on a carbon support. The PEMFC performance was lower than that of a conventional Nafion impregnated electrode because of the lower proton conductivity of SiO_2, nevertheless this type of ceramic carbon electrode is believed to be promising for high temperature (>80 °C) applications due to its water retention capability. By incorporating a water transfer region in the electrodes, Wang et al. [12] proposed another inexpensive and easy method of modifi-

* Corresponding author at: Applied Catalysis, Institute of Chemical and Engineering Sciences, 1 Pesek Road, Jurong Island, Singapore 627833, Singapore.
Tel.: +65 6796 3807; fax: +65 6316 6182.
E-mail address: lin_jianyi@ices.a-star.edu.sg (J. Lin).

0378-7753/$ – see front matter © 2010 Elsevier B.V. All rights reserved.
doi:10.1016/j.jpowsour.2010.06.103

cation of the electrodes without additives; but the incorporation of a water transfer region in the AB-PEMFC means an increase in cell area, which is not favourable for portable devices.

Without external humidification, portable fuel cells are prone to dry out during operation and this leads to lower performance during steady-state operations. To solve this problem, a self-humidifying catalyst using citric acid treatment was fabricated and the performance of the catalyst was evaluated. In previous work [13], citric acid treatment was demonstrated to be a simple and effective method for modifying carbon black and for enhancing the electrochemical activity of Pt catalysts for methanol oxidation. A self-humidifying Pt catalyst with citric acid modified carbon black (CA-CB) as the support was prepared for a H_2 AB-PEMFC. The MEA fabricated from the self-humidifying catalyst is shown to be able to retain water in the reaction regions, thus leading to an enhancement of proton conductivity without addition of hygroscopic oxides or modification to the membrane or electrodes. When a thick polymer membrane NRE212 was used, a Pt/CA-CB catalyst achieved 23.4% higher output power density than that of a commercial catalyst under similar testing conditions (oblique slit cathodes). The method is relatively simple and inexpensive compared with other self-humidifying MEAs reported in the literature, showing a potential application in the enhancement of fuel cell performance in portable devices. A similar approach whereby enhancement of proton conductivity was achieved by modification of the support has been reported by other groups of researchers. For instance, Jia et al. [14] could enhance the wetting of the catalyst layer by oxidation of Pt/C using nitric acid. Instead of using strong acid as the oxidant, Xu et al. [15] and Du et al. [16] employed a simple yet effective method, i.e., thermal decomposition of ammonium sulfate, to attach sulfonic groups on catalyst layers and to improve the conductivity. These methods are similar to the citric acid modification method discussed here.

2. Experimental

2.1. Catalyst preparation

The self-humidifying catalyst was prepared by deposition of Pt nanoparticles on functionalized carbon black, which was derived from commercial carbon black (Vulcan XC72R, Cabot Corp.) using citric acid (CA) treatment as described in a previous publication [13]. In a typical experiment, 100 mg of XC72 carbon black (Cabot Corp.), 100 mg of citric acid monohydrate (Fluka 99.5%) and 10 ml of distilled water were mixed with the assistance of ultrasonic vibration (Elma, 100 W and 35 kHz) for 15 min, and then left to dry to form a paste. After heating at 300 °C for 30 min, the CA-treated carbon black was ready for Pt deposition. The functionalized carbon black is assigned as CA-CB. Pt nanoparticles were subsequently deposited on CA-CB using microwave-assisted heating [17]. Briefly, a 150 mg sample of CA-CB was dispersed in 50 ml of ethylene glycol (EG) by ultrasound treatment in a beaker. An EG solution of $H_2PtCl_6{\cdot}6H_2O$ (Fluka), containing 100 mg of Pt, was added drop-wise to the homogeneous CA-CB in EG solution to obtain a catalyst with 40 wt.% Pt. The mixture of Pt precursor and CA-CB EG solutions was stirred for 20 min. Subsequently, 1 M NaOH in EG solution was added drop-wise to adjust the pH of the mixture to 11 while the total volume of the mixture solution was 150 ml. The mixture solution was then transferred into a round bottom flask and placed inside a microwave reactor (Milestone MicroSYNTH, 2.45 GHz) for 5 min microwave irradiation at 800 W. The resulting suspension of Pt-deposited carbon was centrifuged, washed to remove the organic solvent, and dried at 80 °C overnight in a vacuum oven. The catalyst so prepared is assigned as Pt/CA-CB.

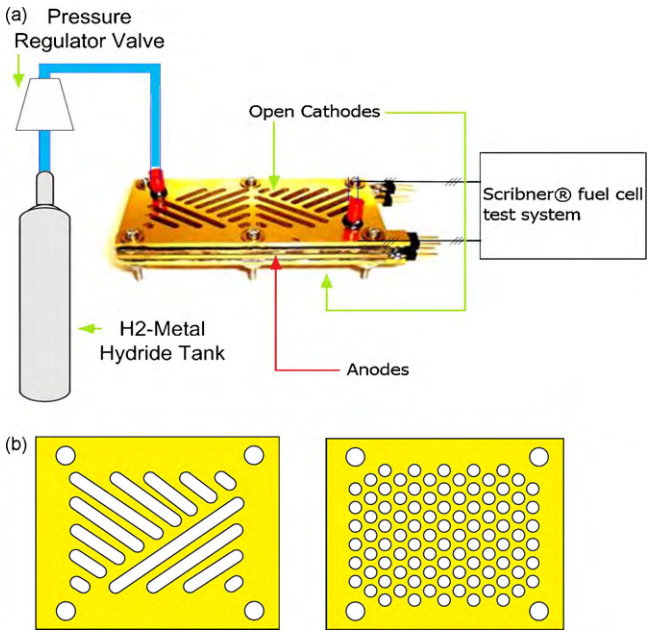

Fig. 1. (a) Schematic illustration of experimental setup for air-breathing PEMFC testing. (b) Two open cathode designs: oblique slit (left) and circular opening (right).

2.2. Catalyst characterization

The distribution and morphology of Pt catalysts were examined by TEM (JEOL JEM 2010F) operated at 200 kV. X-ray diffraction patterns were taken on a Bruker D8 advance X-ray diffractometer, with a 2θ angular range from 10° to 90°. The average crystallite size of the Pt particles was estimated from the diffraction peak of Pt(2 2 0) using the Debye–Scherrer equation [18]. Fourier transformed infrared (FT-IR) transmission spectra were obtained with an EXCALIBUR FTS3000MX FT-IR spectrophotometer in the 4000–400 cm^{-1} region. Cyclic voltammograms (CVs) were recorded at room temperature (25 °C) using an Autolab PGSTAT302 potentiostat/galvanostat and a conventional three-electrode cell that contained a 0.5 M H_2SO_4 electrolyte, a 5 mm diameter glassy carbon working electrode, a platinum foil counter electrode, and an Ag|AgCl reference electrode. The catalyst ink was casted on the glassy carbon electrode in the form of a 5 wt.% Nafion (Aldrich) solution with a metal loading of 407 μg cm^{-2}.

2.3. Fabrication and characterization of air-breathing PEMFCs

The air-breathing PEMFC was fabricated following procedures similar to those described in [19]. The gas diffusion layer (GDL) was prepared by using carbon paper (P75T from Ballard®), Vulcan XC-72R carbon powder (Cabot Co.) and polytetrafluoroethylene (PTFE, 60 wt.% Aldrich), with a 30 wt.% PTFE content and a 1.5 mg cm^{-2} carbon loading. The catalyst layer was deposited on the GDL, and consisted of a 1:1 weight ratio mixture of the Pt/CA-CB catalyst and Nafion (Dupont®), the Pt loading was 0.4 mg cm^{-2}. The 5-layer sandwiched MEA consisted of GDL|Catalyst|Nafion Membrane|Catalyst|GDL and was fabricated by hot-pressing at 50 kg cm^{-2} and 140 °C. For comparison, two types of Nafion membrane (NRE211 or NRE212) were used in separate testsp; NRE212 is 50 μm in thickness while NRE211 is only 25 μm. A MEA with an active area of 11 cm^2 was inserted into an AB-PEMFC test fixture that consisted of two cell stacks, as schematically shown in Fig. 1. Two air-breathing cathodes were positioned on top and bottom of the planar stack. Two anodes were placed back-to-back with an insulation layer separating them (see [19]). The hydrogen flow was

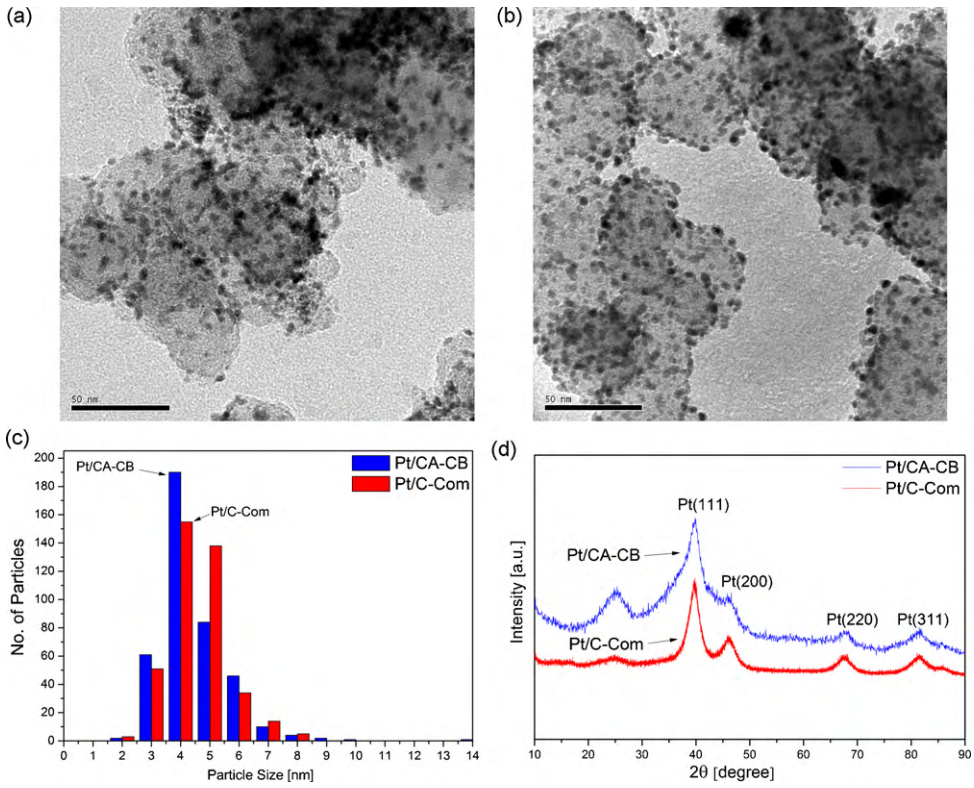

Fig. 2. Size distributions of Pt nanoparticles supported on Vulcan XC72R: (a) TEM image of commercial catalyst Pt/C-Com; (b) TEM of Pt/CA-CB; (c) histograms of particles-size distribution derived from TEM studies of Pt/CA-CB (blue) and Pt/C-Com (red); (d) X-ray diffractograms of Pt/CA-CB (blue) and Pt/C-Com (red). Incident wavelength is 1.5406 Å (Cu Kα). (For interpretation of the references to color in this figure legend, the reader is referred to the web version of this article.)

admitted into the middle plates and distributed to the two cells. Note that two different designs for the open cathode (see Fig. 1b), namely, oblique slit and circular opening, were used in comparative testing to investigate the effect of current density on the water management of the fuel cell.

Polarization curves were measured using a Scribner® fuel cell test system. Cell conditioning was performed at room temperature under a constant voltage of 0.5 V for 2 h prior to data acquisition. Dry hydrogen was fed into anode in a dead-ended mode at a pressure of 20 kPa, while oxygen was diffused by free convection from the surrounding air at room temperature (25 °C) with a relative humidity of 60%.

For comparison with PE/CA-CB, parallel experiments were performed on a commercial Pt/C catalyst purchased from Alfa Aesar (HiSPEC 4000, 40 wt.% Pt supported on Carbon Black), which is labeled as Pt/C-Com in the following text and figures.

3. Results and discussion

3.1. Physical and electrochemical analysis of catalyst

The TEM images in Fig. 2 show that both the commercial catalyst Pt/C-Com (Fig. 2a) and the Pt/CA-CB catalyst (Fig. 2b) have good Pt distribution with a particle size between 2 and 6 nm (Fig. 2c). The average particle sizes for Pt/CA-CB and Pt/C-Com are very similar, i.e., 3.9 and 4.0 nm, respectively.

XRD patterns of the above two samples are compared in Fig. 2d. The peaks at 2θ values of about 39.8°, 46.3°, 67.6°, and 81.5° are characteristic of face-centered cubic (fcc) crystalline Pt, ascribed to the (1 1 1), (2 0 0), (2 2 0), and (3 1 1) planes, respectively. The Pt particle sizes, calculated from the Pt(2 2 0) peak width using the Debye–Scherrer equation are about 3.8 and 4.1 nm for Pt/CA-CB and Pt/C-Com, respectively, that is, in close agreement to the TEM measurements. It is important to note that Pt/CA-CB has much more intense C (0 0 2) peak at 25°, and this implies a better graphitic structure of CA-CB as compared with XC-72 without citric acid treatments. The high crystallinity of carbon is significantly important for good corrosion resistance and hence a long life span of the PEMFC Pt/C catalysts [20].

The citric acid functionalization method modifies the surface of carbon blacks with hydroxyl (–OH), carboxyl (–COOH) and carbonyl (–CO) groups. The FT-IR spectra in Fig. 3 exhibit carbonyl, carboxyl and hydroxyl bands in the regions 1300–1700 and 3300–3600 cm^{-1} for Pt/CA-CB and CA-CB, which are almost negligible for Pt/C-Com and as-purchased XC72R. These functional groups can be also attached on carbon materials by means of chemical oxidation meth-

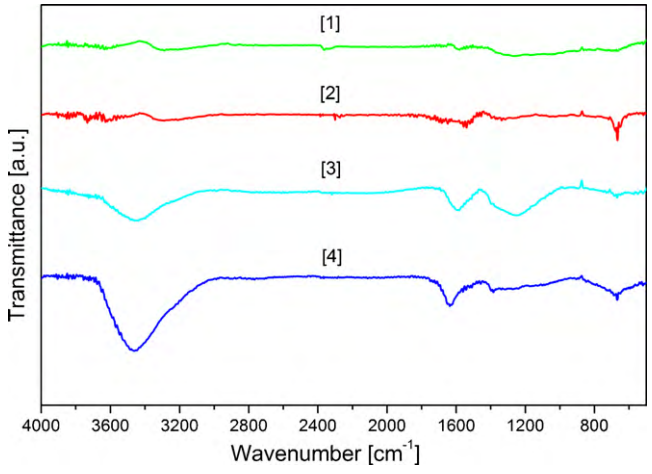

Fig. 3. Infrared transmittance spectra of supported Pt/C catalysts and carbon supports: [1] as-purchased Vulcan XC-72R; [2] Pt/C-Com; [3] CA-CB; [4] Pt/CA-CB.

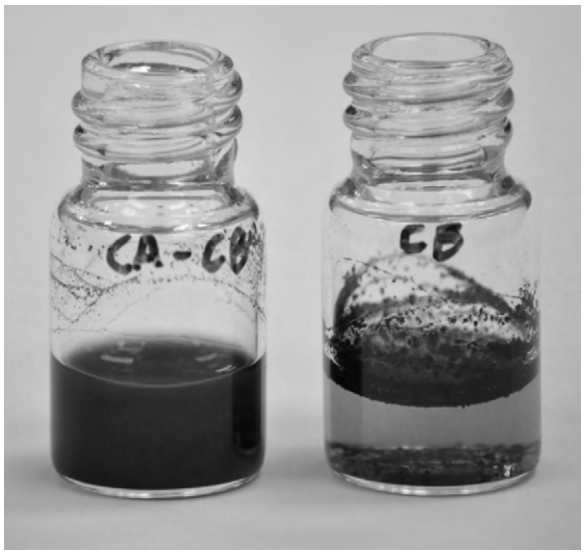

Fig. 4. Comparison of dispersion of 10 mg of citric acid treated XC-72R (CA-CB) and as-purchased Vulcan XC-72R (CB) in de-ionized water after ultrasound treatment for 30 s.

ods that use oxidizing chemicals or acids such as HNO_3, $KMnO_4$, H_2O_2 and H_2SO_4, These methods, however, often require extensive (usually 4–48 h [21–23]) heating during the oxidation process, and a filtration and washing process to remove residue oxidants are also time consuming. In contrast to conventional surface oxidation methods, citric acid funtionalization is simple and fast without prolong heating, and does not require filtration and washing for removal of residue. Citric acid will decompose to carbon dioxide and water when heated above 175 °C at atmospheric pressure, thus citric acid modification method does not require any process for the removal of residue reactant. The citric acid molecule contains three carboxylic groups and one hydroxyl group. During the heating process, the citric acid molecules attached on carbon particles will partially decompose into carboxylic and hydroxyl functional groups that attached to the carbon surface, while those citric acid molecules that are not in contact with the carbon surface will decompose to carbon dioxide and water. It is favourable to maximize the contact of citric acid with the carbon blacks by adding some water to the citric acid and carbon black mixture to form a paste and then rapidly transferring the paste to a furnace preheated at 300 °C.

The presence of functional groups on CA-CB can greatly increase the dispersion of the carbon support in water as demonstrated in Fig. 4. On the other hand, XC72R carbon blacks without functionalization cluster together and separate from the water. The fast dispersion of CA-CB in water indicates that CA-CB is more hydrophilic than its untreated counterpart.

The CV curves for Pt/CA-CB and Pt/C-Com in Fig. 5 are almost the same. The peak at 0.123 V and the shoulder at 0.181 V are attributed to the desorption charge of H_{ads} on Pt(1 1 0) sites, while the peak at 0.243 V is assigned to the desorption charge of H_{ads} on Pt(1 0 0) [24]. Using the hydrogen monolayer adsorption charge of 0.210 μC cm^{-2} on a smooth Pt surface, electrochemical surface areas (ECSA) for the catalysts were calculated from the area enclosed by the hydrogen adsorption and desorption peaks in the CV curves. The ECSA of Pt/CA-CB is calculated to be 53.8 m^2 g^{-1}, i.e., slightly larger than that of Pt/C-Com, which is about 45.8 m^2 g^{-1}.

The physical and electrochemical properties of the two samples obtained from TEM, XRD and CV studies are summarized in Table 1, showing that Pt/CA-CB and Pt/C-Com have similar average Pt particle size and similar ECSA, nevertheless Pt/CA-CB possesses

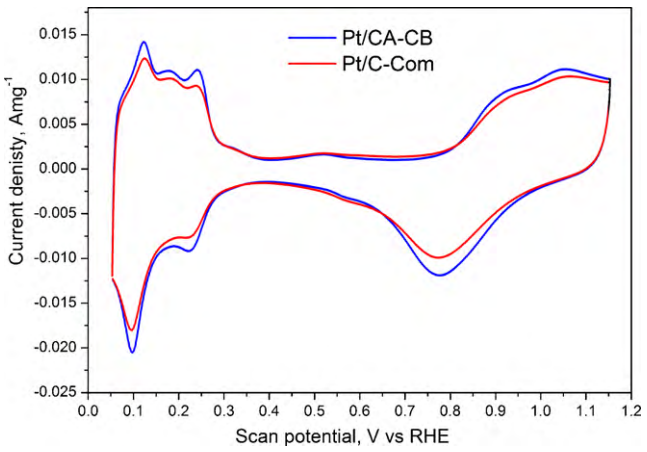

Fig. 5. Cyclic voltammtry (CV) curves of Pt catalysts supported on commercial carbon, Pt/C-Com and Pt on citric acid modified catalyst Pt/CA-CB.

a many more functional groups, and hence higher wettability, than Pt/C-Com.

3.2. Performance evaluation of air-breathing PEM fuel cells (AB-PEMFC)

Fig. 6a displays the polarization curves of the four AB-PEMFCs using different catalysts (i.e., Pt/CA-CB (■) or Pt/C-Com (▲)), and electrolyte membrane (i.e., NRE 211 (green and pink in color) or NRE 212 (blue and red in color)). When the thin membrane NRE 211 is used, the performance of Pt/CA-CB is slightly better than that of Pt/C-Com, with a maximum power density of 101.3 mW cm^{-2} at 0.41 V vs. 96.2 mW cm^{-2} at 0.38 V (see Fig. 6b). This result is consistent with the similar Pt dispersion and electrochemical properties of the two catalysts. When the thick membrane NRE 212 is used the performance of Pt/C-Com/NRE212 is becomes inferior to that of Pt/C-Com/NRE211, particularly at low cell voltage and in the high current region ($V < 0.5\,V$ and $I > 150$ mA cm^{-2}, the region of concentration polarization). The maximum power density is 102.8 mW cm^{-2} at 0.40 V for Pt/CA-CB vs. 83.3 mW cm^{-2} at 0.43 V for Pt/C-Com. All preparation and testing conditions are identical in the two series of experiments, except for the thickness of the membranes, which is 50 μm for NRE 212 and 25 μm for NRE 211.

Water transport and distribution are critical for PEMFCs, in particular for AB-PEMFCs. An appropriate humidity condition not only can improve the performance and efficiency of a fuel cell, but can also prevent irreversible degradation of the catalyst and the membrane. The water content in the MEA can be affected by two processes during fuel cell operation: (i) electro-osmotic drag as the result of protons moving from the anode to the cathode, which pull water molecules along with them and dehydrates the anode; and (ii) back diffusion from cathode to anode, driven by the water concentration gradient across the membrane due to water production at the cathode. The former one is proportional to the proton flow and thus increases with increasing current density, whereas the latter usually predominates and decreases with increasing membrane thickness. The experimental results with NRE 211 in Fig. 6a and b have shown that self-humidification without external humid-

Table 1
Physical and electrochemical properties of 40 wt.% Pt/CA-CB and 40 wt.% Pt/C-Com.

	Particle size from TEM [nm]	Particle size from XRD [nm]	EAS [m^2 g^{-1}]
Pt-CA-CB	3.9	3.8	53.8
Pt/C-Com	4.0	4.1	45.8

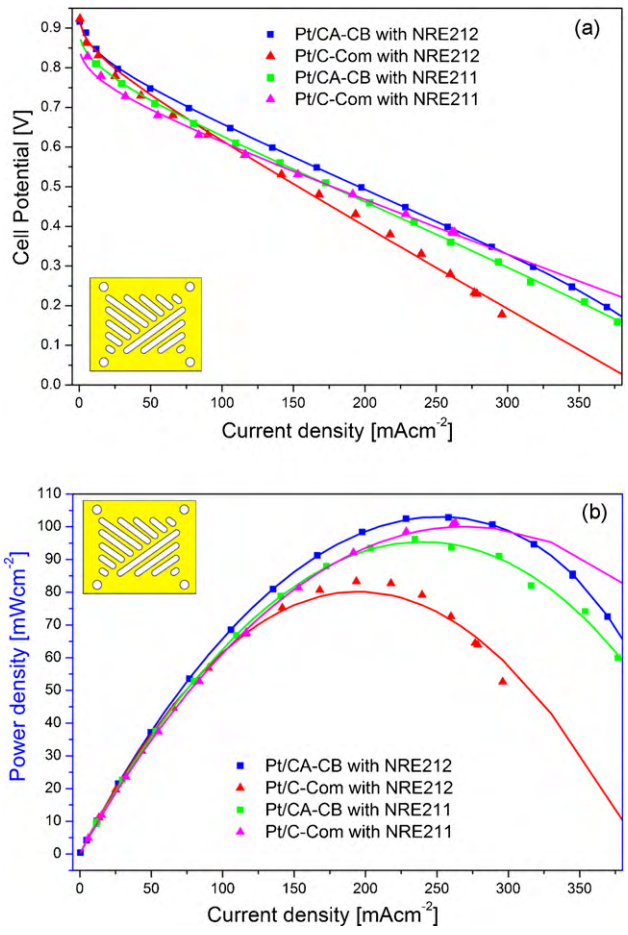

Fig. 6. (a) Polarization curves of Pt/CA-CB and Pt/C-Com catalysts on AB-PEMFC stack with oblique slit cathodes (see schematic diagram in inset) employing Nafion® membrane NRE 212 (■ and ▲) and NRE 211 (■ and ▲), respectively. Solid lines are corresponding fits for experimental data. (b) Power densities curves of four MEAs consisting of Pt/CA-CB and Pt/C-Com with NRE212 and NRE211, respectively.

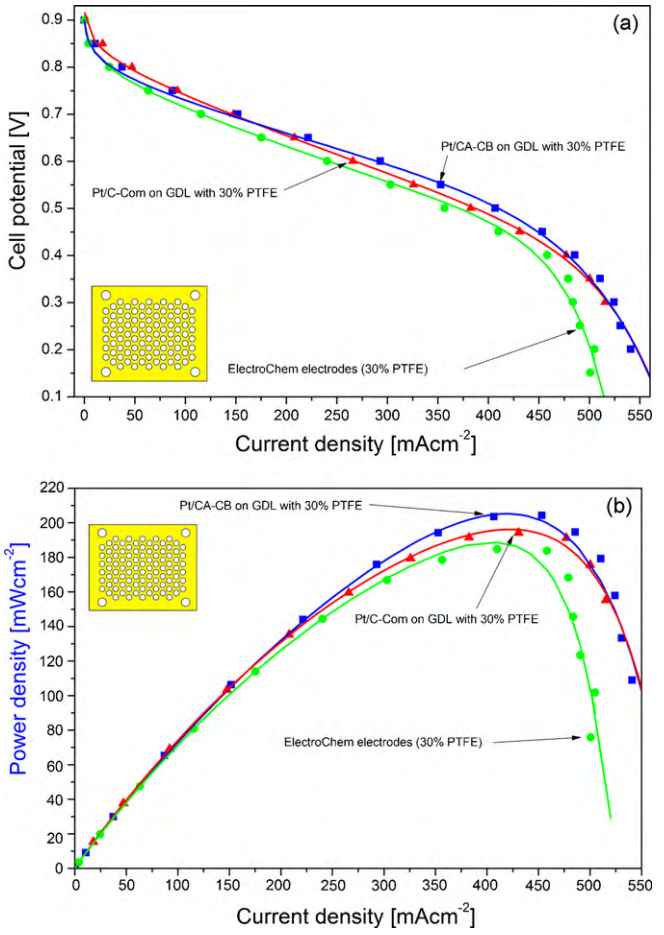

Fig. 7. (a) Polarization curves of Pt/CA-CB and Pt/C-Com with circular opening cathodes, NRE212 membrane and 30 wt% PTFE GDL. Data obtained from ElectroChem Pt/C catalysts under identical conditions are included as reference. (b) Power density curves of Pt/CA-CB and Pt/C-Com with circular opening cathodes, NRE212 membrane and GDL with 30 wt% PTFE.

ifiers for both hydrogen and air works well with both Pt/C-Com and Pt/CA-CB, nevertheless the back-diffusion is obviously weakened with NRE 212 where the thickness is twice of NRE 211. On one hand this may avoid water flooding and pore blocking, but on the other hand the net water loss in the anode region may result in poorer Pt/C-Com fuel cell performance. In this scenario, the hydrophilic property and better water retention capability of Pt/CA-CB can compensate the water loss at the anode and maintain the high performance of the catalyst, as indicated in Fig. 6a and b.

Note that the above data were collected with an oblique slit open cathode and a GDL composed of 30 wt.% PTFE. To study further the effect of catalyst self-humidifying on fuel cell water management, an alternative open cathode design: circular opening design was used for the comparison. Both designs were manufactured with the same opening ratio of 47% [19], but the circular opening design has a shorter rib distance and smaller hydraulic diameter compared with the oblique slit design. A narrower ribbed cathode channel is found to have a better oxygen distribution, while a smaller hydraulic diameter could increase the mass-transfer coefficient. Hence a circular opening design has been shown to perform better than the oblique slit design [19]. This is true for Pt/CA-CB too.

Polarization curves obtained from the AB-PEMFC with a circular opening cathode, a NRE212 membrane and 30 wt.% PTFE GDL are presented in Fig. 7a. The performance is better when a circular opening cathode is used instead of oblique slit cathode. Pt/CA-CB exhibits the highest output power density 204.4 mW cm^{-2} at 0.45 V compared with 194.2 mW cm^{-2} at 0.45 V for Pt/C-Com, both of which are much better than those with oblique slit cathodes in Fig. 6b: 102.8 mW cm^{-2} at 0.40 V for Pt/CA-CB and 83.3 mW cm^{-2} at 0.43 V for Pt/C-Com. The improvement by using circular opening design is more evident for Pt/C-Com because more efficient oxygen diffusion (hence more water production at cathode) with the circular opening design can enhance the water back-diffusion which is weakened due to the use of a thicker membrane (NRE212). In Fig. 7b, the data for ElectroChem electrodes is included as a reference. Its maximum power density is 183.8 mW cm^{-2} at 0.40 V, i.e., less than that for both Pt/CA-CB and Pt/C-Com.

The amount of PTFE content in the GDL can greatly affect the water transportation and diffusion in the MEA and hence greatly influence the fuel cell performance. In Fig. 8a, the polarization curves of the MEAs using GDL with 10 wt.% PTFE (and NRE212, circular opening cathode) give significantly lower current density than those using GDL with 30 wt.% PTFE, including Pt/CA-CB-30%PTFE, Pt/C-Com-30%PTFE and Electro-Chem. This is due to a lesser amount of hydrophobic pores that function as the water removal channels in the GDLs with 10 wt.% PTFE. In this case, the hydrophilic characteristic of Pt/CA-CB is not favourable when the water removal capability of the GDL is lower. The MEA prepared with Pt/CA-CB and 10 wt.% PTFE GDL has a slightly lower performance (166.1 mW cm^{-2} at 0.45 V, see Fig. 8b) compared with that prepared with Pt/C-Com and 10 wt.% PTFE GDL (169.9 mW cm^{-2} at 0.45 V, see Fig. 8b). This clearly demonstrates that to enhance the

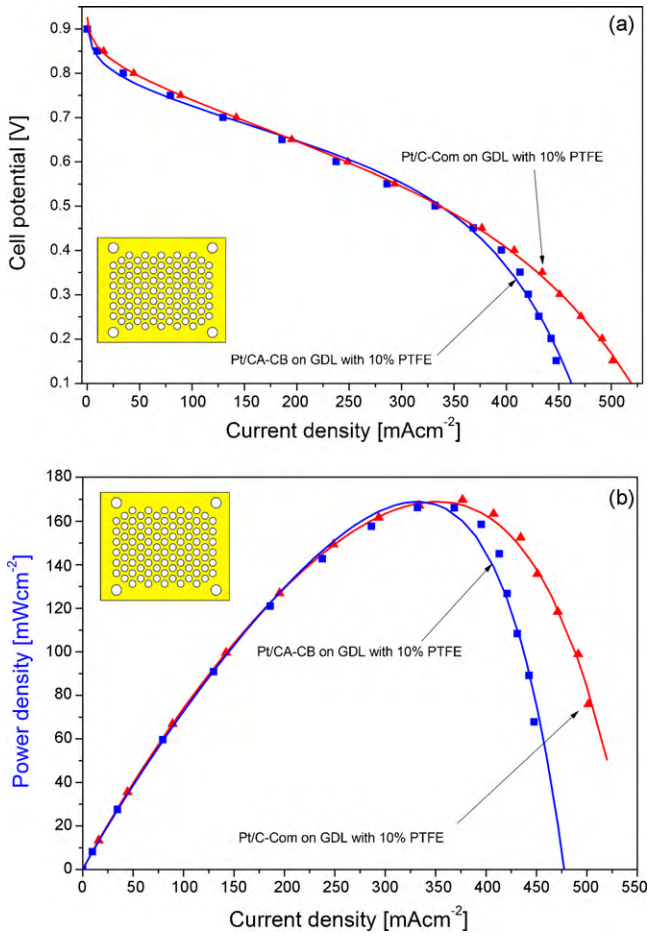

Fig. 8. (a) Polarization curves of Pt/CA-CB and Pt/C-Com fabricated on GDL with 10% PTFE (using NRE212 and circular opening cathode). (b) Power densities curves of Pt/CA-CB and Pt/C-Com fabricated on GDL with 10% PTFE (using NRE212 and circular opening cathode).

performance of MEA in AB-PEMFC, the hydrophilic/hydrophobic properties for both the catalyst layer and the GDL have to be adjusted to obtain optimum performance.

3.3. Simulation analysis of the air-breathing PEM fuel cells (AB-PEMFC)

The polarization curve of a PEMFC can be described by the analytical expression:

$$V = E_r - \eta_{act} - \eta_{ohm} - \eta_{conc} \quad (1)$$

where $E_r(V)$ is the reversible potential for the cell, η_{act} is the activation overpotential, η_{ohm} is the ohmic overpotential (both ionic and ohmic), and η_{conc} is the concentration overpotential. These overpotentials can be expressed as function of current density [25], i.e.,

$$\eta_{act} = b \log_{10}\left(\frac{i + i_{loss}}{i_0}\right) \quad (2)$$

$$\eta_{ohm} = ri \quad (3)$$

$$\eta_{conc} = mie^{ni} \quad (4)$$

where:

$$b = \frac{2.3RT}{\alpha F} \quad (5)$$

and i_0 (mA cm^{-2}) is the exchange-current density; b (V(decade)$^{-1}$) is the Tafel parameter, r (Ω cm^2) is the total cell internal resistance; i_{loss} is the internal current density loss (mA cm^{-2}); α is the transfer coefficient; R (8.314 J mol^{-1} K^{-1}) is the gas constant; F is the Faraday (96,485 C mo1^{-1}) constant; T (K) is the temperature. Parameters m (Ω cm^2) and n (cm^2 mA^{-1}) are empirical curve-fitting parameters for the exponential voltage drop observed in the high current density region.

A modified logarithmic charge-transfer overpotential fitting term (Eq. (2)), incorporating a fitted exchange-current density as well as a fitted internal cell current density as proposed in Ref. [26] was utilized here. A modification of the concentration overpotential term proposed by Kim et al. [27] by multiplication of the current density (Eq. (4)) was implemented in this study. The modification of the concentration overpotential term was corrected according to the considerations suggested by Xia and Chan [28], namely, that mass-transport losses should occur in all ranges of current density and should be proportionally dependent on current density.

Combining Eqs. (1)–(4), a semi-empirical current voltage equation is obtained:

$$V = E_r - b \log_{10}\left(\frac{i + i_{loss}}{i_0}\right) - ri - mie^{ni} \quad (6)$$

and when $i = 0$, Eq. (6) gives the open-circuit potential,

$$E_{ocv} = E_r - b \log_{10}\left(\frac{i_{loss}}{i_0}\right) \quad (7)$$

For analysis of the polarization curves, another kinetic parameter, viz., the mass-transfer impedance (R_m), was implemented and the equation takes the form:

$$R_m = \frac{\eta_{conc}}{i} = me^{ni} \quad (8)$$

Since the fitting parameters m and n are not derived from any physical or chemical consideration, it makes more sense to discuss the mass-transfer impedance as the parameter that is capable of describing the exponential voltage drop in the polarization curve.

A non-linear least-squares method was employed to fit the polarization curves (solid lines in Fig. 6a) to the semi-empirical current–voltage equation. The fitted parameters are given in Tables 2 and 3. The correlation coefficient obtained from the non-linear least-squares fitting is in excess of 0.99.

The temperature-dependent theoretical reversible potential for the cell is given by [29,30]:

$$E_r = 1.229 - 8.5 \times 10^{-3}(T - 298.15) + \frac{RT}{2F} \ln[p_{H_2}(p_{O_2})^{0.5}] \quad (9)$$

where p_{H_2} and p_{O_2} are the partial pressure of H_2 and O_2, respectively. At $T = 298.15$ K, $E_r = 1.221$ V, which is about 0.1 V higher than the fitting results (ca. 1.1 V, from Tables 2 and 3). This may be due to the increase in cell temperature during the measurements, especially at high current densities; the cell temperature may rise to

Table 2
Electrode-kinetic and mass-transfer parameters for MEAs tested using oblique slit cathodes. Same GDL with 30% PTFE content used for all MEAs.

	E_r [V]	E_{ocv} [V]	b [V(decade)$^{-1}$]	i_{loss} [mA cm^{-1}]	i_0 [10^{-6} A cm^{-2}]	r [Ω cm^2]	m [Ω cm^2]	n [cm^2 mA^{-1}]	R^2
Pt/CA-CB with N212	1.103	0.9316	0.05954	0.7900	1.044	1.473	0.000065	0.0194200	0.9995
Pt/C-Com with N212	1.092	0.9319	0.05544	0.7865	1.019	1.987	0.001600	0.0008960	0.9972
Pt/CA-CB with N211	1.096	0.8839	0.06513	1.802	0.9990	1.384	0.024340	0.0044000	0.9997
Pt/C-Com with N211	1.046	0.8453	0.06081	1.964	0.9820	1.273	0.003010	0.0000025	0.9979

Table 3
Electrode-kinetic and mass-transfer parameters for MEAs tested using circular opening cathodes. NRE 212 used for all MEAs.

	E_r [V]	E_{ocv} [V]	b [V(decade)$^{-1}$]	i_{loss} [mA cm^{-2}]	i_0 [10^{-6} A cm^{-2}]	r [Ω cm^2]	m [Ω cm^2]	n [cm^2 mA^{-1}]	R^2
Pt/CA-CB on GDL with 30% PTFE	1.075	0.9002	0.05888	0.9680	1.040	0.513	0.000520	0.0124400	0.9962
Pt/C-Com on GDL with 30% PTFE	1.084	0.9215	0.05501	0.9500	1.057	0.692	0.000044	0.0164100	0.9985
Pt/CA-CB on GDL with 10% PTFE	1.104	0.9119	0.06507	0.9330	1.042	0.519	0.004370	0.0114200	0.9961
Pt/C-Com on GDL with 10% PTFE	1.099	0.9291	0.05751	0.8996	0.9996	0.690	0.010200	0.0078500	0.9989
ElectroChem electrodes	1.092	0.9113	0.06294	0.7394	0.9966	0.632	0.000003	0.0240700	0.9932

ca. 40 °C. If T = 313.15 K (i.e., 40 °C) is substituted in Eq. (9), the theoretical reversible potential will be 1.093 V and the fitted E_r values for the MEAs are similar to this value. The Tafel slopes for the MEAs are well within the range reported in the literature from 0.052 V(decade)$^{-1}$ to 0.096 V(decade)$^{-1}$ [26–28,31,32]. The value of 0.06 V(decade)$^{-1}$, which is a typical low Tafel slope value, corresponds to a regime where O_2 reduction occurs on a Pt oxide covered surface [33], as a consequence of low current density due to low temperature and humidification. The fitted internal current density loss i_{loss} is similar to values reported in the literature [34–36] that are in the range of 1–2 mA cm^{-2}. The fitted open-circuit potential (OCV) for the MEAs also gives a value that is close to the actual OCV measured. From comparison of the results reported in the literature with the parameters in Table 2, it can be concluded that the parameters obtained through numerical fitting using the semi-empirical current–voltage equation are reasonable representatives of the electrochemical properties of the cells. All MEAs have a similar reversible potential E_r, open-circuit potential E_{OCV}, exchange-current density i_0 and Tafel slope b. This demonstrates that the electrochemistry and the catalyst utilization rate are similar and the difference in their performance is mainly attributed to physical properties. The exchange-current density for PEMFC has been reported to range from 1×10^{-4} to 4.84×10^{-8} A cm^{-2} [37–42], whereas the exchange-current densities of the MEAs obtained from the numerical procedure are around 1.0×10^{-6} A cm^{-2}, which is in the lower side of the above-mentioned i_0 range reported by other workers. This is reasonable as the polarization curves are obtained from AB-PEMFC operating at room temperature, and the low ambient temperature and oxygen flux are the causes of smaller exchange-current density [33]. The i_{loss} for MEAs with NRE 211 is about double that of MEAs with NRE 212 (1.8 mA cm^{-2} vs. 0.8 mA cm^{-2}). This is consistent with the fact that NRE 212 is twice as thick as the NRE 211 and thus able to reduce the crossover of H_2 that contributes to internal current losses. The resistance r of the cells obtained from the numerical procedures is found to range from 0.5 to 2 Ω cm^2. For MEAs using the oblique slit cathode, the resistance for Pt/CA-CB is around 1.38–1.47 Ω cm^2, i.e., similar to that reported by Chu and Jiang [43], i.e., 1.33 Ω cm^2 for a 32-cm^2 cell operating at 30 °C and 50% relative humidity. The Pt/C-Com with NRE212 has the largest resistance r (1.987 Ω cm^2), in agreement with the argument that it has the least water content in the membrane due to poor back-diffusion and low humidification.

The effect of the hydrophilic catalyst Pt/CA-CB on the performance improvement is reflected in the lower resistance of the cell compared with one with the catalyst Pt/C-Com (1.473/1.987; 0.513/0.692; 0.519/0.690 in Tables 2 and 3). That is, the ability to retain water in the catalyst layer can reduce the internal resistance of the cell. The ohmic overvoltage can be written as:

$$\eta_{ohm} = ri = (r^{el} + r^{ion})i \quad (10)$$

The electronic resistance r^{el} is negligible, whereas, the ionic resistance r^{ion} depends greatly on the degree of humidification of the membrane and catalyst layer [44–47], the dynamic electro-osmotic drag and the back-diffusion processes of water. In Table 2, which lists the electrokinetic parameters for the MEAs with oblique slit cathodes, the resistance of the MEA using commercial Pt/C-Com and NRE211 is 1.273 Ω cm^2. When NRE 212 is used, the resistance of the Pt/C-Com MEA is increased to 1.987 Ω cm^2. The increment in resistance can be attributed to the increase of the membrane thickness (from 25.4 μm for NRE 211 to 50.8 μm for NRE 212) that impedes the back diffusion of water. The decrease in water content in the membrane and catalyst layer causes the drop in ionic conduction and is reflected as an increase in cell resistance. On the other hand, the MEA resistance of the catalyst Pt/CA-CB with NRE 212 is about 1.473 Ω cm^2, which only increased by about 6.4% from 1.384 Ω cm^2 when NRE 211 was used for the MEA. This demonstrates that the water retention ability of the Pt/CA-CB catalyst is able to maintain a higher ionic conductivity compared to Pt/C-Com when a thicker membrane is used. When a thinner membrane is employed, the performance of Pt/C-Com and Pt/CA-CB is similar, since a thinner membrane would be beneficial for water back-diffusion and would facilitate the hydration of the membrane and thus the advantage of using a hydrophilic catalyst does not prevail [45,46].

When the circular opening design is used for the cathode, the cell resistance for the MEAs in Table 3 is significantly smaller than those using oblique slit cathodes, in the range between 0.513 and 0.69 Ω cm^2. The reduction in cell resistance is due to greatly improved diffusion and transportation of oxygen. As a result, more water generation, as well as more water transport by proton from anode (electro-osmotic water drag) [47], would hydrate the membrane and catalyst layers, lowering the ionic resistance. The experimental results in Ref. [47] indicate that when the cathode is not humidified, at high current densities the net electro-osmotic drag coefficient (net number of water molecules carried by each proton) has a larger value. That is with the circular opening cathode (higher current density than oblique slit cathode) water dry out in the anode region may occur, and the self-humidifying Pt/CA-CB can hence have more water content and lower resistance than Pt/C-Com.

When GDLs with less PTFE loading (10 wt.% vs. 30 wt.%) are used in the MEAs, larger mass-transfer impedance is seen in Fig. 9, particularly at high current densities. The finding is in agreement with

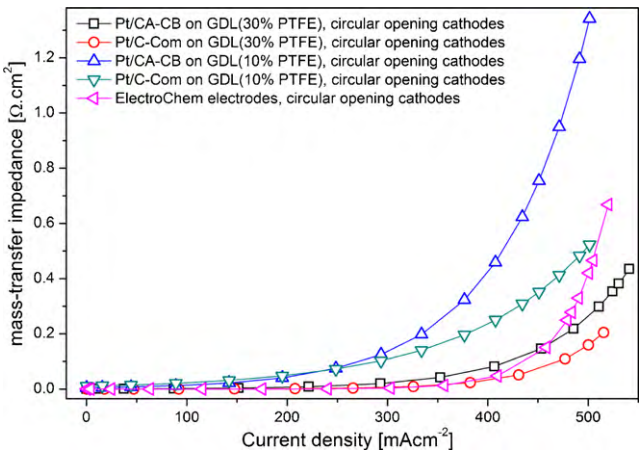

Fig. 9. Mass-transfer impedance for polarization curves of AB-PEMFC with circular opening design.

the experimentally observed large potential drop in the high current density region due to the use of GDLs with 10 wt.% PTFE. This is a consequence of flooding in the electrodes due to less hydrophobic pores to allow transport of oxidant to the reaction sites. In this case, the performance of Pt/CA-CB is worse than that of Pt/C-Com since both the catalyst layers and the GDLs of the MEA are hydrophilic.

4. Conclusions

In summary, a 40 wt.% Pt/C catalyst, Pt/CA-CB prepared by using citric acid functionalized carbon black (CA-CB) as the support shows an effective self-humidifying property in AB-PEMFC. Pt/CA-CB has similar physical and electrochemical properties to a commercial catalyst Pt/C-Com, but has a highly hydrophilic property and exhibits excellent performance in air-breathing PEMFC stack. When a thin polymer membrane NRE211 is used as the solid electrolyte, Pt/CA-CB and Pt/C-Com show little difference in fuel cell performance. On the other hand, when a thicker polymer membrane (NRE212) is used as the electrolyte, Pt/CA-CB-NRE212 gives a power output of 102 mW cm^{-2}, which is 23.4% higher than that from the commercial catalyst Pt/C-Com-NRE212 under similar testing conditions. This result is particularly useful when it applies to a working environment with low ventilation and humidity. Although a thinner membrane can be used to increase back-diffusion of water, a thicker membrane still prevails if durability is considered; hence Pt/CA-CB will be useful to increase the ionic conductivity while maintaining cell durability. Under better oxygen transport conditions using an improved cathode design (circle opening), a MEA with the combination of Pt/CA-CB, NRE212 and GDL with 30 wt.% PTFE shows an even higher performance, with 204 mW cm^{-2} at 0.45 V, i.e., better than that of Pt/C-Com, NRE212 and GDL with 30 wt.% PTFE (191 mW cm^{-2} at 0.40 V). Simulation analysis of the polarization curves with semi-empirical current–voltage equations reveals that the self-humidifying Pt/CA-CB catalyst possesses high water retention capability and is able to maintain the hydration level of the membrane, and thereby reduces the internal cell resistance. This result is especially useful for portable applications of PEMFCs, in which self-humidification and air-breathing are both essential, and it has potential commercial value, since the CA modification approach is simple, effective, and of low cost.

Acknowledgement

The authors are grateful for financial support from the Science and Engineering Research Council (SERC) of the Agency for Science, Technology and Research (A*STAR) of Singapore.

References

[1] C.K. Dyer, J. Power Sources 106 (2002) 31–34.
[2] C. Bia, H. Zhang, Y. Zhang, X. Zhu, Y. Ma, H. Dai, S. Xiao, J. Power Sources 184 (2008) 197–203.
[3] T. Yang, Int. J. Hydrogen Energy 33 (2008) 2530–2535.
[4] Y. Liu, T. Nguyen, N. Kristian, Y. Yu, X. Wang, J. Membr. Sci. 330 (2009) 357–362.
[5] Y.-H. Liu, B. Yi, Z.-G. Shao, L. Wang, D. Xing, H. Zhang, J. Power Sources 163 (2007) 807–813.
[6] W. Zhang, M.K.S. Li, P.-L. Yue, P. Gao, Langmuir 24 (2008) 2663–2670.
[7] H. Uchida, Y. Ueno, H. Hagihara, M. Watanabe, J. Electrochem. Soc. 150 (2003) A57.
[8] Y. Zhang, H. Zhang, Y. Zhai, X. Zhua, C. Bi, J. Power Sources 168 (2007) 323–329.
[9] M. Han, S.H. Chan, S.P. Jiang, Int. J. Hydrogen Energy 32 (2007) 385–391.
[10] U.H. Jung, S.U. Jeong, K.T. Park, H.M. Lee, K. Chun, D. Choi, S.H. Kim, Int. J. Hydrogen Energy 32 (2007) 4459–4465.
[11] J.I. Eastcott, E.B. Easton, Electrochim. Acta 54 (2009) 3460–3466.
[12] E.-D. Wang, P.-F. Shi, C.-Y. Du, J. Power Sources 175 (2008) 183–188.
[13] C.K. Poh, S.H. Lim, H. Pan, J. Lin, J.Y. Lee, J. Power Sources 176 (2008) 70–75.
[14] N. Jia, R.B. Martin, Z. Qi, M.C. Lefebvre, P.G. Pickup, Electrochim. Acta 46 (2001) 2863–2869.
[15] Z.Q. Xu, Z.G. Qi, A. Kaufman, Electrochem. Solid-State Lett. 8 (2005) A313–A315.
[16] C.Y. Du, T.S. Zhao, Z.X. Liang, J. Power Sources 176 (2008) 9–15.
[17] J. Zeng, F. Su, Y.-F. Han, Z. Tian, C.K. Poh, Z. Liu, J. Lin, J.Y. Lee, X.S. Zhao, J. Phys. Chem. C 112 (2008) 15908–15914.
[18] E. Antolini, F. Cardellini, J. Alloys Compd. 315 (2001) 118–122.
[19] N. Bussayajarn, M. Han, K.H. Kwan, Stephen, Y.M. Wan, S.H. Chan, Int. J. Hydrogen Energy 34 (2009) 7761–7767.
[20] F.D. Negra, M. Meneghetti, E. Menna Fullerenes, Nanotubes Carbon Nanostruct. 11 (2003) 25–34.
[21] Y. Xing, J. Phys. Chem. B 108 (2004) 19255–19259.
[22] J. Zhang, H. Zou, Q. Qing, Y. Yang, Q. Li, Z. Liu, X. Guo, Z. Du, J. Phys. Chem. B 107 (2003) 3712–3718.
[23] V. Lordi, N. Yao, J. Wei, Chem. Mater. 13 (2001) 733–737.
[24] J. Solla-Gullón, P. Rodríguez, E. Herrero, A. Aldaz, J.M. Feliu, Phys. Chem. Chem. Phys. 10 (2008) 1359–1373.
[25] F. Barbir, PEM Fuel Cells: Theory and Practice, Elsevier-Academic Press, 2005, p. 49.
[26] S.D. Fraser, V. Hacker, J. Appl. Electrochem. 38 (2008) 451–456.
[27] J. Kim, S.-M. Lee, S. Srinivasan, C.E. Chamberlin, J. Electrochem. Soc. 142 (1995) 2670–2674.
[28] Z.T. Xia, S.H. Chan, Int. J. Hydrogen Energy 32 (2007) 878–885.
[29] M.J. Khan, M.T. Iqbal, Fuel Cells 4 (2005) 463–475.
[30] J.C Amphlett, R.M. Baumert, R.F. Mann, B.A. Peppley, P.R. Roberge, J. Electrochem. Soc. 142 (1995) 1–8.
[31] D. Chu, R. Jiang, C. Walker, J. Appl. Electrochem. 30 (2000) 365–370.
[32] G. Squadrito, G. Maggio, E. Passalacqua, F. Lufrano, A. Patti, J. Appl. Electrochem. 29 (1999) 1449–1455.
[33] A. Parthasarathy, S. Supramaniam, A.J. Appleby, C.R. Martin, J. Electrochem. Soc. 139 (1992) 2530–2537.
[34] V. Ramani, H.R. Kunz, J.M. Fenton, J. Membr. Sci. 232 (2004) 31–44.
[35] S. Shyam, J. Kocha, Y. Deliang, S.Yi. Jung, AIChE J. 52 (2006) 1916–1925.
[36] V. Ramani, H.R. Kunz, J.M. Fenton, Electrochim. Acta 50 (2005) 1181–1187.
[37] J. Larminie, A. Dicks, Fuel Cell Systems Explained, John Wiley & Sons Ltd., Chichester, GB, 2000, p. 52.
[38] J.H. Nam, M. Kaviany, Int. J. Heat Mass Transfer 46 (2003) 4595–4611.
[39] J.C. Amphlett, R.M. Baumert, R.F. Mann, B.A. Peppley, P.R. Roberge, J. Electrochem. Soc. 142 (1995) 1–15.
[40] L. You, H. Liu, Int. J. Hydrogen Energy 26 (2001) 991–999.
[41] L. You, H. Liu, Int. J. Heat Mass Transfer 45 (2002) 2277–2287.
[42] D. Bevers, M. Wohr, K. Yasuda, K. Oguro, J. Appl. Electrochem. 27 (1997) 1254–1264.
[43] D. Chu, R. Jiang, J. Power Sources 83 (1999) 128–133.
[44] M.G. Santarelli, M.F. Torchio, P. Cochis, J. Power Sources 159 (2006) 824–835.
[45] M. Paquin, L.G. Fréchette, J. Power Sources 180 (2008) 440–451.
[46] S.H. Chan, M. Han, S.P. Jiang, J. Electrochem. Soc. 154 (2007) B486–B493.
[47] K. Choi, D. Peck, C.S. Kim, D. Shin, T. Lee, J. Power Sources 86 (2000) 197–201.